$Na_2K_{21}Tl_{19}$, a Novel Thallium Compound Containing Isolated Tl_5^{7-} and Tl_9^{9-} Groups. A New Hypoelectronic Cluster

Zhenchao Dong and John D. Corbett*

Contribution from the Ames Laboratory—DOE[1] and Department of Chemistry, Iowa State University, Ames, Iowa 50011

Received December 6, 1993®

Abstract: The title compound is synthesized in high yield by fusion of the elements in sealed Ta containers followed by slow cooling to and annealing at 250 °C. The structure was established by single crystal means (*Cmcm*, $Z = 4$, $a = 11.345$ (2) Å, $b = 13.807$ (3) Å, $c = 41.832$ (8) Å, $R/R_w = 5.3/4.3\%$). The independent unit contains two Tl_5 and one Tl_9 units ordered in layers and well separated by the cations which bond to, and bridge between, faces, edges, and vertices of the clusters. The sodium appears essential in this role. The former cluster, a distorted trigonal bipyramid (C_m symmetry), is proportioned as is Pb_5^{2-}, etc. and should be analogously formulated as the isoelectronic Tl_5^{7-} according to EHMO calculations. The new Tl_9 geometry (C_{2v}, d(Tl–Tl) = 3.13–3.44 Å) can be obtained by substantial elongation of two side edges of a tricapped trigonal prism (D_{3h}) so that the intervening face-capping atom moves close to that face and becomes eight-bonded. MO calculations illustrate how this distortion of either Bi_9^{5+}- or $B_9H_9^{2-}$-like polyhedra affords a hypoelectronic state for Tl_9^{9-} ($2n$ skeletal electrons). More direct geometric and electronic relationships are found on removal of four adjoining vertices from a centered icosahedral Tl_{13}. The compound is diamagnetic and a very poor conductor ($\rho_{293} \sim 800$ $\mu\Omega$·cm).

Introduction

Four kinds of larger isolated clusters have been found for thallium in addition to the Tl_2 dimers present in Li_5Tl_2[2] and Sr_5Tl_3 (Cr_5B_3 type).[3] One is the classical tetrahedral Tl_4^{8-} anion in Na_2Tl,[4] which has 12 skeletal electrons and is isoelectronic and isosteric with Pb_4^{4-} and P_4. Two relatively recent additions are (a) the 18-electron, hypoelectronic, pentacapped trigonal prismatic Tl_{11}^{7-} ions in A_8Tl_{11}, A = K, Rb, Cs,[5,6] metallic solids comparable to K_8In_{11}[7] and (b) the analogous, tetragonally-compressed "octahedra" Tl_6^{6-} in KTl.[8] Finally, $Tl_{10}Zn^{8-}$, a discrete, bicapped square antiprism of Tl centered by Zn, is present in $K_8Tl_{10}Zn$[6] in a phase that is isostructural with $K_8In_{10}Zn$.[9] Some extended three-dimensional network structures also exist. The best known is the stuffed diamond array found in NaTl (d(Tl–Tl) = 3.24 Å) where the thallium sublattice was aptly described as $^3_\infty[Tl^{-1}]$ by its discoverers Zintl and Dullenkopf.[10] A few extended structures that contain linked icosahedra, pentagonal antiprisms, and hexagonal antiprisms of thallium have also been identified recently.[6]

We report here on the novel "naked" clusters Tl_5^{7-} and Tl_9^{9-} that occur in the phase $Na_2K_{21}Tl_{19}$. Both can be understood with relatively simple bonding pictures, the first according to Wade's rules[11] and the second, as another hypoelectronic version of more conventional clusters but in a new geometry. The new compound nicely illustrates how delicately size factors and electronic requirements can combine to create an unprecedented three-dimensional structure in which new cluster anions have been trapped.

Experimental Section

Syntheses. The title compound was obtained unexpectedly from a reaction designed for the preparation of KTl, evidently because of a mix-up of reagents. The pure phase was later synthesized from the constituent elements in a reaction with the stoichiometry determined by a single crystal X-ray structural analysis. Because both reactants and the product are very sensitive to air and moisture, all handling operations were performed in a glovebox in a N_2 atmosphere with humidity less than 0.01 ppm vol. The surfaces of the Na (99.9%, Alpha), K (99.9%, Baker), and Tl (99.998%, Johnson-Mathey) metals were cleaned with a scalpel before weighing and transfer. An ~250-mg mixture was placed in a tantalum tube (3/8 inch o.d.) already welded at one end, and this was tightly crimped and arc welded under a He atmosphere. The container was then sealed in a fused silica jacket under high vacuum and heated in a tubular furnace. The samples were initially homogenized in the liquid state at 500 °C for 15 h, slowly cooled to 250 °C at a rate of 5 deg/h and equilibrated at this temperature for 15 days, and finally cooled to room temperature at a rate of 3 deg/h. The new phase is exceedingly brittle, and the black crystalline fragments exhibit bright metal-like surfaces. EDAX (energy dispersive analysis by X-ray) results on several crystals confirmed the presence of Na, K, and Tl atoms and gave compositions close to the $Na_2K_{21}Tl_{19}$ deduced by crystallography. The structure is not formed from thallium plus ~1:10 mixtures of either Na–Rb or K–Rb cations.

X-ray Powder Diffraction. X-ray powder patterns were collected under vacuum from finely ground samples that had been mounted between pieces of cellophane tape. An Enraf-Nonius Guinier camera with Cu Kα radiation ($\lambda = 1.540\,562$ Å) and NBS (NIST) silicon as an internal standard were employed for this purpose. The powder pattern calculated on the basis of the refined structural model matched the observed one very well, and least-squares refinement of 55 measured 2θ values together with their indices and those of the standard Si lines resulted in orthorhombic cell dimensions of $a = 11.345(2)$ Å, $b = 13.807(3)$ Å, $c = 41.832(8)$ Å, and $V = 6553(2)$ Å^3.

Physical Properties. The resistivity of the phase was examined by the electrodeless "Q" method[12] for two samples of ~80 and ~85 mg that were sieved to 250–400 μm powders and mixed with Al_2O_3. Measurements were made at 35 MHz over the range of 153–293 K. Magnetic susceptibility data were obtained from a 28.4-mg ground sample of the title compound sealed under He in the container type described elsewhere.[13] Magnetization data were measured at a field of 3 T over the range of

• Abstract published in *Advance ACS Abstracts,* March 15, 1994.
(1) The Ames Laboratory is operated for U.S. Department of Energy by Iowa State University under Contract No. W-7405-Eng-82. This research was supported by the Office of the Basic Energy Sciences, Materials Sciences Division, DOE.
(2) Stöhr, J.; Schäfer, H. *Z. Naturforsch.* **1979**, *34B*, 653.
(3) Bruzzone, G.; Franceschi, E.; Merlo, F. *J. Less-Common Met.* **1978**, *60*, 59.
(4) Hansen, D. A.; Smith, J. F. *Acta Crystallogr.* **1967**, *22*, 836.
(5) Cordier, G.; Müller, V. *Z. Kristallogr.* **1992**, *198*, 281.
(6) Dong, Z. C.; Corbett, J. D. Unpublished research.
(7) Sevov, S. C.; Corbett, J. D. *Inorg. Chem.* **1991**, *30*, 4875.
(8) Dong, Z. C.; Corbett, J. D. *J. Am. Chem. Soc.* **1993**, *115*, 11299.
(9) Sevov, S. C.; Corbett, J. D. *Inorg. Chem.* **1993**, *32*, 1059.
(10) Zintl, E.; Dullenkopf, W. *Z. Physik. Chem.* **1932**, *B16*, 195.
(11) Wade, K. *Adv. Inorg. Chem. Radiochem.* **1976**, *18*, 1.
(12) (a) Shinar, J.; Dehner, B.; Beaudry, B. J.; Peterson, D. T. *Phys. Rev.* **1988**, *37B*, 2066. (b) El-Hanany, U. *Rev. Sci. Instrum.* **1973**, *44*, 1067.
(13) Sevov, S. C.; Corbett, J. D. *Inorg. Chem.* **1992**, *31*, 1895.

0002-7863/94/1516-3429$04.50/0

Table 1. Selected Data Collection and Refinement Parameters for $Na_2K_{21}Tl_{19}$

space group, Z	*Cmcm* (no. 63), 4
lattice parameters,[a] Å	
a	11.345 (2)
b	13.807 (3)
c	41.832(8)
vol, Å^3	6553(2)
no. indep. obs. refl. ($I > 3\sigma(I)$), variables	1492, 117
μ, cm^{-1} (Mo Kα)	483.55
residuals, R, R_w[b]	0.053, 0.043

[a] Guinier data, λ = 1.540 562 Å, 20 °C. [b] $R = \sum||F_o| - |F_c||/\sum|F_o|$; $R_w = [\sum w(|F_o| - |F_c|)^2/\sum w(F_o)^2]^{1/2}$, $w = \sigma_F^{-2}$.

6–300 K on a Quantum Design MPMS SQUID magnetometer. The raw data were corrected for the susceptibility of the container and for atom core diamagnetism.[14]

Structure Determination. Many well-formed crystals of the major phase were obtained from the initial reaction. Several plate-like members were sealed in thin-walled capillaries, and Laue, oscillation, and Weissenberg photographs were used to check the singularity of crystals and possible space group assignments. A single crystal with dimensions ca. 0.5 × 0.3 × 0.1 mm was chosen for data collection, which was carried out at room temperature on CAD4 single crystal diffractometer with the aid of graphite-monochromated Mo Kα radiation. A C-centered orthorhombic cell with lattice constants as expected from the film studies was obtained on programmed indexing of 25 reflections from a random search over $14° \le 2\theta \le 30°$. One octant of data was collected with the C-centered absences imposed. The data were corrected for Lorentz and polarization effects and for the strong absorption (μ = 484 cm^{-1}) with the aid of the average of five ψ-scans of reflections at different θ values. Both the film results and the reduced data were consistent with only two space groups, *Cmcm* (no. 63) and $Cmc2_1$ (no. 36). The Wilson statistics suggested a centrosymmetric space group, and hence the former was chosen for the first and successful trial. Selected details of the data collection and refinement are listed in Table 1.

Application of the direct methods[15] gave eight apparent heavy atom positions plus others with heights only about 25% of the first set. Interatomic distances among the former ranged between 3.0 and 3.5 Å, typical for Tl–Tl distances. These were therefore so assigned for the first few cycles of least-squares refinements. (All calculations were performed using the TEXSAN package.[16]) The subsequent difference Fourier synthesis revealed nine additional peaks, seven of which could be assigned as K without any difficulty on consideration of probable K–Tl and K–K distances. Sodium was assigned to a smaller peak with distances of 3.1–3.25 Å to Tl and of 3.5–3.8 Å to K. The ninth position (K8) had one short contact to Tl2, 3.37 Å, but all other distances were normal. Refinement with isotropic thermal parameters proceeded smoothly, and a DIFABS empirical absorption correction[17] applied after convergence lowered R from 13 to 8%. The K8 atom lay very close to the special position 4*c* (*m2m*; 0, *y*, 1/4) with a *z* coordinate that produced a pair of atoms separated by 0.99(5) Å. After anisotropic refinement, a multiplicity variation for K8 with all other atoms fixed indicated that each site is 50.0(1)% occupied. Similar procedures applied to the occupancy refinements for Tl, Na, and all other K atoms (in parts) indicated that these sites were fully occupied as the deviations from unity were all less than 3σ, and they were so fixed thereafter. The anisotropic refinement, including a secondary extinction correction, converged with the residuals $R(F)$ = 5.3%, $R_w(F)$ = 4.3%, and GOF = 1.55. The highest residual peak in the final difference Fourier map was 2.83 e$^-$/Å^3, 1.10 Å from Tl2. The R_{int} value of 7.0% for observed data and a somewhat larger-than-normal residual peak in the final difference Fourier map were likely both influenced by the high absorption and the small number of duplicate reflections (~100), and their limited distribution in reciprocal space as these affected the absorption correction.

K8 is the only atom in this structure that might suggest a possible noncentric symmetry. Its position has *m2m* symmetry, and removal of the 2-fold axis along *b* and the mirror perpendicular to *c* would reduce the group symmetry to $Cmc2_1$ (no. 36) and eliminate the split position for K8. However, the solution and refinement of the structure in this

(14) Selwood, P. W. *Magnetochemistry*, 2nd ed.; Interscience Publishers: New York, 1956; p 70.
(15) SHELXS-86, Sheldrick, G. M. Universität Göttingen, Germany, 1986.
(16) TEXSAN, version 6.0 package, Molecular Structure Corp.: The Woodlands, TX, 1990.
(17) Walker, N.; Stuart, D. *Acta Crystallogr.* **1983**, *A39*, 158.

Table 2. Interatomic Distances (Å) in $Na_2K_{21}Tl_{19}$ (<5 Å)

			Tl 1		
Tl1	3.418(5)	Tl 4	2 × 3.316(2)	K6	3.95(2)
Tl2	3.438(3)	K1	2 × 3.696(9)	K7	4.24(2)
Tl 3	2 × 3.275(2)	K5	2 × 3.550(9)		
			Tl 2		
Tl 1	2 × 3.438(3)	Tl 4	4 × 3.128(2)	K8	3.37(2)
Tl3	2 × 3.228(2)	K1	2 × 3.78(1)		
			Tl 3		
Tl 1	2 × 3.275(2)	K1	3.49(1)	K7	2 × 4.50(1)
Tl 2	3.228(2)	K1	3.54(1)	K8	3.53(1)
Tl 4	2 × 3.302(2)	K5	2 × 3.81(1)		
			Tl 4		
Tl 1	3.316(2)	K1	3.689(7)	K6	3.93(1)
Tl 2	3.128(2)	K4	3.95(1)	K7	4.063(2)
Tl 3	3.302(2)	K5	3.874(9)	K8	4.49(2)
Tl 4	3.223(2)	K5	3.634(9)	Na	3.22(2)
			Tl 5		
Tl 6	3.405(3)	K2	3.97(1)	K3	2 × 3.84(1)
Tl 7	3.164(4)	K2	3.67(2)	K4	2 × 3.98(1)
Tl 8	2 × 3.251(2)	K3	2 × 3.953(8)		
			Tl 6		
Tl 5	3.405(3)	K3	2 × 3.809(9)	K6	4.76(2)
Tl 7	3.537(3)	K3	2 × 3.81(1)	Na	3.13(2)
Tl 8	2 × 3.072(2)	K4	2 × 4.053(9)		
			Tl 7		
Tl 5	3.164(4)	K4	2 × 3.598(8)	K7	3.66(2)
Tl 6	3.537(3)	K5	2 × 3.581(9)	Na	3.11(2)
Tl8	2 × 3.111(2)				
			Tl 8		
Tl 5	3.251(2)	K2	3.795(9)	K4	3.641(9)
Tl 6	3.072(2)	K3	3.73(1)	K5	3.89(1)
Tl 7	3.111(2)	K3	3.85(1)	K6	3.806 (9)
Tl 8	4.906 (2)	K4	3.692(9)	Na	4.04(2)
			K1		
Tl 1	2 × 3.696(9)	Tl 3	3.54(1)	K5	2 × 4.03(1)
Tl 2	3.77(1)	Tl 4	2 × 3.689(7)	K7	2 × 3.93(2)
Tl 3	3.49(1)	K1	4.42(2)	K8	3.95(2)
			K2		
Tl 5	3.67(2)	K2	4.08(3)	K4	2 × 4.09(2)
Tl 5	3.97(1)	K3	2 × 4.42(1)	K6	4.02(2)
Tl 8	2 × 3.795(9)	K3	2 × 4.38(1)		
			K3		
Tl 5	3.953(8)	Tl 8	3.73(1)	K3	3.95(1)
Tl 5	3.84(1)	Tl 8	3.85(1)	K3	3.91(2)
Tl 6	3.809(9)	K2	4.42(1)	K3	3.85(2)
Tl 6	3.81(1)	K2	4.38(1)	K4	3.95(2)
			K4		
Tl 4	3.95(1)	Tl 8	3.641(9)	K5	4.59(1)
Tl 5	3.98(1)	K2	4.09(2)	K6	4.13(1)
Tl 6	4.053(9)	K3	3.95(2)	K7	4.24(2)
Tl7	3.598(8)	K5	4.34(1)	Na	3.75(1)
Tl 8	3.692(9)				
			K5		
Tl1	3.550(9)	Tl 8	3.89(1)	K6	3.92(1)
Tl 3	3.81(1)	K1	4.03(1)	K7	4.27(2)
Tl 4	3.874(9)	K4	4.34(1)	K8	3.95(2)
Tl 4	3.634(9)	K4	4.59(1)	Na	3.58(2)
Tl 7	3.581(9)				
			K6		
Tl 1	3.95(2)	Tl 8	2 × 3.806(9)	K5	2 × 3.92(1)
Tl 4	2 × 3.93(1)	K2	4.02(2)	Na	3.81(3)
Tl 6	4.76(2)	K4	2 × 4.13(1)		
			K7		
Tl 1	4.24(2)	Tl 7	3.66(2)	K5	2 × 4.27(2)
Tl 3	2 × 4.50(1)	K1	2 × 3.93(2)	K8	4.08(3)
Tl 4	2 × 4.063(2)	K4	2 × 4.24(2)		
			K8		
Tl 2	3.37(2)	K1	2 × 3.95(2)	K7	4.08(3)
Tl 3	2 × 3.53(1)	K5	2 × 3.95(2)	K8	0.99(5)
Tl 4	2 × 4.49(2)				
			Na		
Tl 4	2 × 3.22(2)	Tl 8	2 × 4.04(2)	K5	2 × 3.58(2)
Tl 6	3.13(3)	K4	2 × 3.75(1)	K6	3.81(3)
Tl 7	3.11(2)				

space group still gave two equal and independent peaks around this position separated by 1.01 Å. There is another possible space group, *A2am* (no. 40); however, structure solution and refinement in this once again resulted in two close, independent peaks in the difference Fourier map. All these factors suggested that the K8 splitting is real, consistent with the coordination environment of the site, as will be described in the next section. It is not surprising that refinements with the above, lower symmetry space groups also resulted in pronounced correlations between appropriate variables for those pairs of atoms that are symmetry equivalent in the centric case.

In order to understand more about both the splitting of the K8 position and the observed property behaviors (below), a data set was also collected at about −60 °C using a smaller crystal, a faster scanning speed, and the same diffractometer. The structure was essentially the same, except that the K8 position could no longer be split but remained fixed at the special position 4*c* (0, *y*, 1/4). However, its anisotropic thermal parameters with a U_{33}/U_{11} ratio of ~15:1 still strongly indicated that the atom was disordered along the [001] direction. The other positional parameters remained within 2σ of those from the earlier study. The ellipsoids were about half as large as before, while the errors were all about 50% larger, presumably because of fewer data (1069 reflections, 115 variables; R/R_w = 0.053/0.052; *a* = 11.276 (3) Å, *b* = 13.702 (2) Å, *c* = 41.553 (3) Å, *V* = 6420 (3) Å^3).

The positional and displacement parameters are contained in the supplementary material. These as well as structure factor data are also available from J.D.C.

Results and Discussion

Structure Description. The most spectacular features of this structure are the coexistence of two separate "naked" thallium cluster anions, Tl_5^{7-} as a distorted trigonal bipyramid and Tl_9^{9-} which can be considered to be a strongly distorted tricapped trigonal prism. The charges (oxidation numbers actually) assigned to the ions correspond to the electron localization expected from properties of the phase and the relative stabilities predicted from calculations (below). Both are the first examples found among the triels Tl, In, Ga, and Al. Isoelectronic, approximately trigonal bipyramidal ions (~D_{3h}) have previously been reported for Sn_5^{2-}, Pb_5^{2-},[18] and Bi_5^{3+},[19] while nothing of the geometric character of Tl_9^{9-} has evidently been seen before. Nine-atom tricapped trigonal prisms (closo, ~D_{3h}) with 20 (or 22) skeletal electrons are known for $B_9H_9^{2-}$,[20] $B_7C_2H_7(CH_3)_2$ (C_{2v}),[21] Ge_9^{2-},[22] and Bi_9^{5+},[23,24] while *nido*-Ge_9^{4-},[22] and Sn^{94-} [25] occur as ~C_{4v} monocapped square antiprisms with the appropriate 22 skeletal electrons.[26]

Each formula unit $Na_2K_{21}Tl_{19}$ contains two Tl_5 and one Tl_9 clusters. The nearest neighbor distances within $Na_2K_{21}Tl_{19}$ are given in Table 2. The former cluster, Figure 1, is apparently derived from the idealized (D_{3h}) trigonal bipyramid but has only exact mirror (C_m) symmetry through the waist atoms Tl5, Tl6, and Tl7. Ranges in equatorial–equatorial and axial–equatorial distances, 0.38 and 0.18 Å, respectively, evidently result from uneven bonding to/distortions by neighboring cations (below). The average values, 3.369(3) and 3.145(2) Å, respectively, correspond to a slightly compressed trigonal bipyramid with the longer distances between the four-bonded waist atoms. If fact, such a geometric feature is remarkably analogous to that in Sn_5^{2-}, Pb_5^{2-}, and Bi_5^{3+}, where the differences between these two types of distances are 0.23, 0.24 and 0.31 Å, respectively, very similar

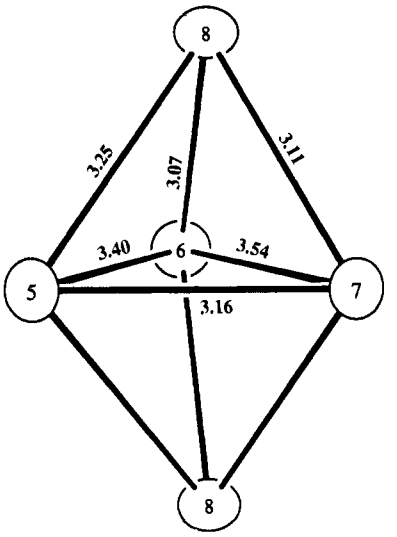

Figure 1. The Tl_5^{7-} cluster unit in $Na_2K_{21}Tl_{19}$, a distorted trigonal bipyramid. (C_m symmetry, 50% thermal displacement ellipsoids for all figures.)

to the 0.22 Å in Tl_5. The intracluster distance Tl8–Tl8, 4.906 Å, is long enough to exclude any significant bonding interaction.

The polyhedron found for Tl_9 is shown in three views in Figure 2. An unambiguous association of this with a familiar, high-symmetry nine-atom reference is difficult thanks to its pronounced distortion. The D_{3h} tricapped trigonal prism and C_{4v} monocapped square antiprism are symmetry limits for common nine-atom polyhedra, with the former generally the electron poorer, and the usual fluxionality observed within examples of the former is generally viewed as proceeding via the latter.[26-28] The nature of the distortion from D_{3h}, Figure 3b, through C_{2v} and toward C_{4v} proceeds along a normal vibration by simple elongation of *one* side edge of the trigonal prism, together with a decrease in the separation between the two adjoining capping atoms, Figure 3a, so that these four atoms eventually define the diagonals of the square base of the new C_{4v} figure. The opposite distortion with *two* prism heights increased and one fixed (or shortened) gives a hitherto unknown C_{2v} intermediate[29] (and an alternate fluxional route[27]). This process clearly seems to lie on the path to the present Tl_9 shown in Figure 2a. In this way, the original tricapped trigonal prism in Figure 3b (numbered according to the new Tl_9) is lengthened along the two Tl4–Tl4 edges and relatively shortened along Tl1–Tl1, Figure 3c. The three former capping atoms become Tl2 and 2Tl3. The C_2 axis through Tl2 that bisects the Tl1–Tl1 edge and the two mirror planes that contain that axis and pairs of Tl3 or Tl1 atoms are retained.

The observed Tl_9 is, however, considerably more distorted than originally visualized for the C_{2v} transition state. Two side edges in the original trigonal prism, Tl4–Tl4, open up greatly to 5.34 Å, but fairly normal distances to the capping Tl2 and Tl3 atoms are preserved, 3.13 and 3.30 Å, respectively, vs an average of 3.27 Å over the polyhedron. As seen better in Figure 2b, the capping Tl2 atom moves to 0.25 Å above the plane of the Tl4 atoms. At the same time, Tl2 also gains four additional neighbors, 2Tl1, the far edge of the original prism, and 2Tl3, the other two face-capping atoms, at 3.44 and 3.23 Å, respectively. The separation between the other face-capping atoms, Tl3–Tl3, remains very long, 5.18 Å.

The dihedral angle criteria[26,27] that are widely considered to be more definitive and expeditious in differentiating polyhedra

(18) Edwards, P. A.; Corbett, J. D. *Inorg. Chem.* **1977**, *16*, 903.
(19) (a) Corbett, J. D. *Inorg. Chem.* **1968**, *7*, 198. (b) Krebs, B.; Mummert, M.; Brendel, C. *J. Less-Common Met.* **1986**, *116*, 159.
(20) Guggenberger, L. J. *Inorg. Chem.* **1968**, *7*, 2260.
(21) Koetzle, T. F.; Scarbrough, F. E.; Lipscomb, W. N. *Inorg. Chem.* **1968**, *7*, 1076.
(22) Belin, C. H. E.; Corbett, J. D.; Cisar, A. *J. Am. Chem. Soc.* **1977**, *99*, 7163.
(23) Hershaft, A.; Corbett, J. D. *Inorg. Chem.* **1963**, *2*, 979.
(24) Friedman, R. M.; Corbett, J. D. *Inorg. Chem.* **1973**, *12*, 1134.
(25) Corbett, J. D.; Edwards, P. A. *J. Chem. Soc., Chem. Commun.* **1975**, 984.
(26) Corbett, J. D. *Chem. Rev.* **1985**, *85*, 383.
(27) Guggenberger, L. J.; Muetterties, E. L. *J. Am. Chem. Soc.*, **1976**, *98*, 7221.
(28) O'Neill, M. E.; Wade, K. *J. Mol. Struct.* **1983**, *103*, 259.
(29) Such a figure is found in $Na_4(en)_7Sn_9$ (Diehl, L., Khodadedeh, K.; Kummer, D.; Strähle, J. *Z. Naturforsch.* **1976**, *31B*, 522), but this particular distortion appears to arise because of interactions of two prismatic edges in Sn_9^{4-} with incompletely ligated sodium ions.[26]

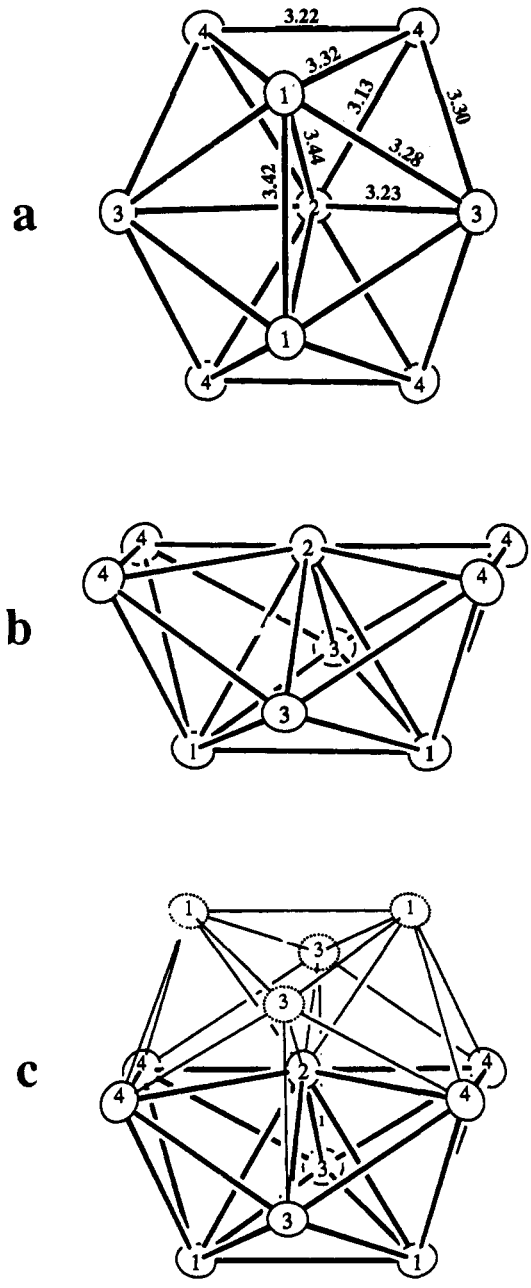

Figure 2. (a,b) Two orthogonal views of Tl_9^{9-} anion (C_{2v}) in $Na_2K_{21}Tl_{19}$, a strongly distorted tricapped trigonal prism. The 2-fold axis and mirror planes lie normal to the page in *a*. (c) The close relationship of the observed species to the centered icosahedral Tl_{13}.

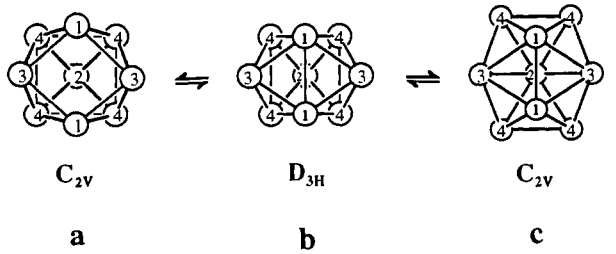

Figure 3. The C_{2v} distortions of a tricapped trigonal prism (D_{3h}, center) toward, left, an unicapped square antiprism (C_{4v}) or, right Tl_9^{9-}, through lengthening of one or two edges of the trigonal prism, respectively.

emphasize how strongly the Tl_9 geometry deviates from the ideal values. Thus, the characteristic vicinal angles defined by capping atoms and the shared edge, e.g., the two 1-3-1 planes in Figure 3b, change from $\delta \sim 22°$ for D_{3h} (Bi_9^{5+} [26]) to 44.3° for the 1-3-1 pair and 51.1° × 2 for 2-4-4 and 3-4-4. Similarly, the parallel triangular ends, for which $\delta = 180°$ in D_{3h}, diverge so that δ becomes 141.4° in Tl_9 (vs 158° in the opposite sense in Sn_9^{4-}, etc.). In spite of the sizable differences, Tl_9 does seem to relate better to the D_{3h} parent than to any other fairly regular nine-atom figure we have found. The average bond lengths about each atom (and the number of neighbors) are Tl1, 3.340 Å (6); Tl2, 3.230 Å (8); Tl3, 3.276 Å (5); and Tl4, 3.242 Å (4). These averages compare with 3.220 Å in Tl_5 as well as 3.18 Å in Tl_6^{6-} (D_{4h}) and 3.24 Å in Tl_4^{8-} with only four-bonded atoms. Longer distances normally follow an increase in the number of bonded neighbors and more delocalization, so that the short bonds about the unique eight-bonded Tl2 are especially remarkable.

The novel Tl_9^{9-} can also be readily derived from a centered icosahedron by removal of four adjoining vertices, as shown in Figure 2c. The polyhedron in Figure 2b is thus also generated from two pentagonal bipyramids defined by axial Tl1 and shared Tl2 that are fused and share both Tl3 and bifunctional Tl1 atoms. This approach proves to be especially useful in electronic descriptions (below). Yet another but seemingly less useful polyhedral description can be found in Figure 2a, a trigonal-bipyramidal Tl_5 unit defined by axial Tl3 and equatorial 2Tl1, Tl2 (with the customarily larger waist distances, 3.43 Å) that is tetracapped by 4Tl4.

Cation Dispositions. Many of the larger, newly discovered naked indium and thallium clusters have relatively low charges and thence fewer countercations per cluster, roughly 8–11.5, and the apparently specific roles of the alkali metal ions about cluster faces, edges and vertices, often in a dual bridging role, have been commented on before. Indeed, the polyhedral choice for $In_{10}Ni^{10-}$ could be rationalized in terms of a need for more faces and longer edges to accommodate the cations.[30] The cation environments about each cluster in the present phase are illustrated in the supplementary material. The trigonal-bipyramial Tl_5 in $Na_2K_{21}Tl_{19}$ is surrounded by 20 alkali-metal atoms. Each axial–equatorial edge is μ_2-bridged by one K atom (Tl5–Tl8, Tl6–Tl8, Tl7–Tl8 by K3, K4, K5, respectively), and the longest equatorial edge Tl6–Tl7 is μ_2-bridged by Na. The four triangular faces meeting at Tl5 are each μ_3-capped by a K3 or K4 atom that is edge-bridging in another Tl_5. Finally, all vertices have two exo-bonded K(2, 3, or 6) atoms, with the exception of Tl7 which has only one exo-bonded K7 atom and this is close only to that thallium. The distortion of Tl_5 is probably related to the foregoing, nonisotropic environment, as with Tl_6^{6-},[8] and smaller deviations are to be expected in the presence of larger alkali-metal cations, as in CsTl.[6]

The surroundings of Tl_9 are a little more complex, with 29 alkali-metal atoms. All triangular faces but two are capped by K atoms. The two edge-shared Tl2–Tl3–Tl4 faces are capped by a single μ_4-K1 atom, while the smaller Tl2–Tl4–Tl4 faces are not capped, rather the short Tl4–Tl4 edges are μ_2-bridged by Na atoms. Tl1, Tl2, and Tl3 each have one exo-bonded K atom, and Tl4, three (K4, 5, 7). Conversely, the overall coordination around Tl1, Tl3, Tl4, and Tl5 is each derived from more or less distorted icosahedra, while Tl2 and Tl8 are 11-coordinated within *nido*-icosahedra, Tl6 centers a bicapped pentagonal prism, and Tl7 is ten-coordinate, all of these being distorted. Compared with other K atoms, K6 and K7 have more open environments in terms of the K–Tl distances around them, and this probably relates to their larger thermal parameters, 5.8 and 7 $Å^2$, respectively, vs 3.5–5.0 $Å^2$ for the rest. For instance, K7 has only one Tl neighbor at <4.00 Å. Each of the split K8 atoms has only three close Tl atoms, being exo to 2Tl3 and particularly close to Tl2 in the same role (at 3.37 vs ≥3.5 Å for the others). The fact that this K8 refines split and 0.5 Å above or below the mirror plane defined by Tl2 and the two Tl3 can be understood to result from the already short K8–Tl2 distance plus the fact that there no other

(30) Sevov, S. C.; Corbett, J. D. *J. Am. Chem. Soc.* **1993**, *115*, 9089.

neighbors beyond this fairly flat face on Tl_9 short of Tl4 at 4.5 Å and two exo K5 and K1 in the same mirror plane and 3.95 Å removed.

The Na atom is tetrahedrally coordinated by four Tl atoms (2Tl4, Tl6, and Tl7). The average Na–Tl distance is 3.17 Å, close to 3.24 Å in NaTl,[10] and the average Na–K distance is 3.69 Å, near the 3.61 Å in KNa_2.[31] Thus the size of this tetrahedral cavity is very appropriate for sodium, but it is presumably too small for a potassium (or another phase is more stable), and the binary $K_{23}Tl_{19}$ does not form. We have repeatedly noted that factors such as this seem particularly important in the stabilization of phases containing diverse networks and new clusters in which the products must satisfy reasonable packing requirements, cation bonding to (solvation of) the cluster anions, and, ultimately, the requisite stoichiometry and cluster electron counts, as will be discussed below.

The overall cluster packing is also very interesting. As shown in a [001] view in Figure 4a, the Tl_9 units are connected in layer through the triangularly coordinated K8 atoms that are bonded exo to Tl2 and 2Tl3. These close-packed, rectangular layers alternate with similar, eclipsed pairs of Tl_5 layers in which the Tl_5 clusters fall directly above and below the K8 atoms. The Tl_5 layers are in turn separated by double K3 (and K2) layers, as can be seen in the [010] side view in Figure 4b. The shortest intercluster distances, Tl6–Tl6 = 5.20 Å, lie across this double K layer, while the next shortest, d(Tl4–Tl7) = 5.50 Å, is also between layers.

Properties and Bonding. Magnetic measurements yielded almost temperature-independent susceptibilities of $-(12.5–13.5) \times 10^{-4}$ emu/mol for the title compound over 6–300 K after container correction. Two types of diamagnetic corrections were applied, as before,[7,8,13] for the contributions from the ionic cores and the Larmor precession of the orbital electrons in each cluster (Langevin contribution). For the latter, we appropriately averaged the distances from the center of each cluster to the middle of the different types of M–M edges on its surface to gain r_{av} assuming no significant further delocalization onto the cations. The ion core corrections totaled 9.29×10^{-4} emu/mol and the Larmor precession, 1.76×10^{-4} emu/mol of $Na_2K_{21}Tl_{19}$. Therefore, the net molar susceptibility χ_M is about $-(1.5–2.5) \times 10^{-4}$ emu/mol, indicating a diamagnetic property. The net value would be a little closer to zero were diamagnetic contributions from the presumed largely lone-pair $6s^2$ valence electrons on thallium to also be included. Resistivity data from two ground samples measured by the Q method over 153–293 K, noisy because of the relatively high resistivities, ranged between ~800 μΩ·cm at the extremes and ~200 μΩ·cm at 243 (±10) K with another possible downturn above ~280 K. The meaning of these possible variations is not clear, but the second structural refinement at ~213 K (Experimental Section) made it clear that the latter two effects do not involve phase transitions. No inflections were observed in the magnetic data either. The resistivities are in any case so large that localization of a very large fraction of the valence electrons is obvious.

Electronic structure calculations were carried out on the isolated Tl_5 and Tl_9 clusters by EHMO methods.[32] Both idealized and real cluster geometries were studied for the sake of comparison and discussion. Atomic parameters employed for thallium and their justification have been described elsewhere.[8] Calculated results for the Tl_5 unit both as observed (C_m) and for the idealized D_{3h} version with average values for the two unique dimensions gave the same bonding conclusions. The Tl_5 trigonal bipyramid exhibits 11 occupied valence orbitals, six bonding skeletal orbitals plus five low-lying members that are mainly 6s pairs on the atoms. The Tl_5^{7-} cluster anion is calculated to have a HOMO–LUMO gap of ~0.86 eV with a 7a′ HOMO level at −5.95 eV. In other

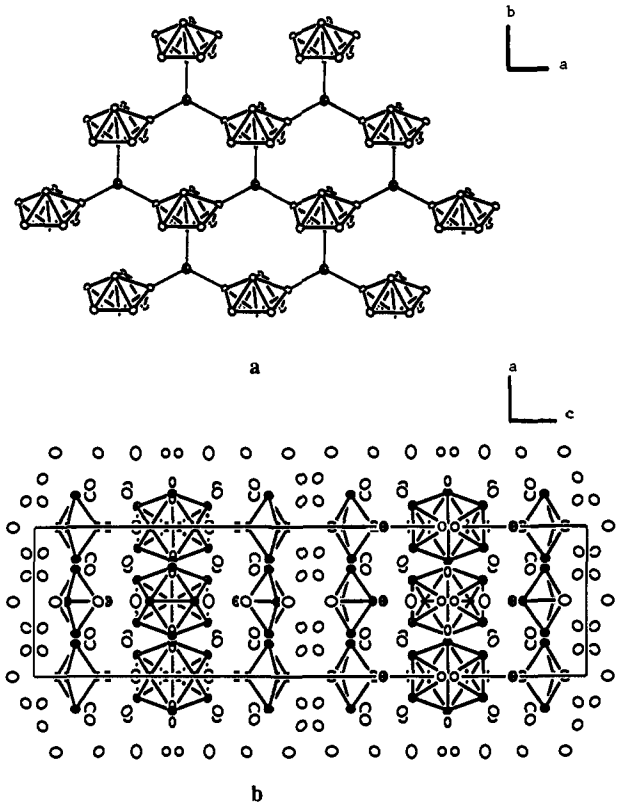

Figure 4. (a) [001] view of a portion of $Na_2K_{21}Tl_{19}$ showing the layers of Tl_9^{9-} (open ellipsoids) interconnected by K8. (b) [010] view illustrating the stacking of Tl_9^{9-}, double Tl_5^{7-} layers, and K^+ and Na^+ ions along c (Tl-shaded, K-open, Na-crossed ellipsoids).

words, the geometrical deviation of Tl_5 from D_{3h} is not caused by, or does not result in, significant electronic variations, but it basically must arise from packing/bonding interactions with the cations. The Tl_5^{7-} example thus provides further testimony for the common characteristics of trigonal-bipyramidal clusters previously represented by Sn_5^{2-}, Pb_5^{2-},[18] and Bi_5^{3+},[19] all of which obey Wade's ($n + 1$) orbital rule.[11] Formal charges in this series can be understood with classic valence rules as well,[33] in the following way: $Tl_5^{7-} \simeq (3b\text{-}Tl^{2-})_2 + (4b\text{-}Tl^{1-})_3$; $Pb_5^{2-} \simeq (3b\text{-}Pb^{1-})_2 + (4b\text{-}Pb^{\circ})_3$; $Bi_5^{3+} \simeq (3b\text{-}Bi^{\circ})_2 + (4b\text{-}Bi^{1+})_3$ where nb means n-bonded. Notice that these descriptions refer to oxidation states, not anything like real charge distributions.

Calculations relating the isolated Tl_9 unit to other nine-atom examples are not as straightforward. Classical tricapped trigonal prismatic (D_{3h}, closo) clusters such as Ge_9^{2-} require $2n + 2 = 20$ skeletal electrons, whereas we appear to have only $2n = 18$ available for the unusually shaped Tl_9^{9-} assuming that Tl_5^{7-} is correctly assigned. (In fact, the isosteric, 22-electron ($2n$+4) but *closo*-Bi_9^{5+} can be rationalized in terms of the fall in energy of the nominal a_2'' LUMO in Ge_9^{2-} and $B_9H_9^{2-}$ when the trigonal prism is elongated so that the ratio of the height:basal edge lengths (h:e) is increased from ~1.0:1 to ~1.15:1.[26,28] An h:e of 1.08 is also sufficient in the $2n + 3$ Sn_9^{3-}.[34]) The study therefore included consideration of the dependence of electron counts on the skeletal distortions in units proportioned more like known species with h:e = 1.15:1 (Bi_9^{5+}) and h:e = 0.97:1 ($B_9H_9^{2-}$) with the basal edges fixed at 3.28 Å. Figure 5 illustrates the essence of these, the MO energies, and symmetries for the skeletal orbitals for the observed C_{2v} Tl_9 cluster (b) and the two D_{3h} models just noted in (a) and (c), respectively. (The nine low-lying and predominantly s-based MOs are not shown for clarity.) The gap

(31) Laves, F.; Walbaum, H. J. *Z. Anorg. Allg. Chem.* **1942**, *250*, 110.
(32) Hoffmann, R. *J. Chem. Phys.* **1963**, *39*, 1397.
(33) von Schnering, H.-G. *Angew. Chem., Int. Ed. Engl.* **1981**, *20*, 33.
(34) Critchlow, S. C.; Corbett, J. D. *J. Am. Chem. Soc.* **1983**, *105*, 5715.

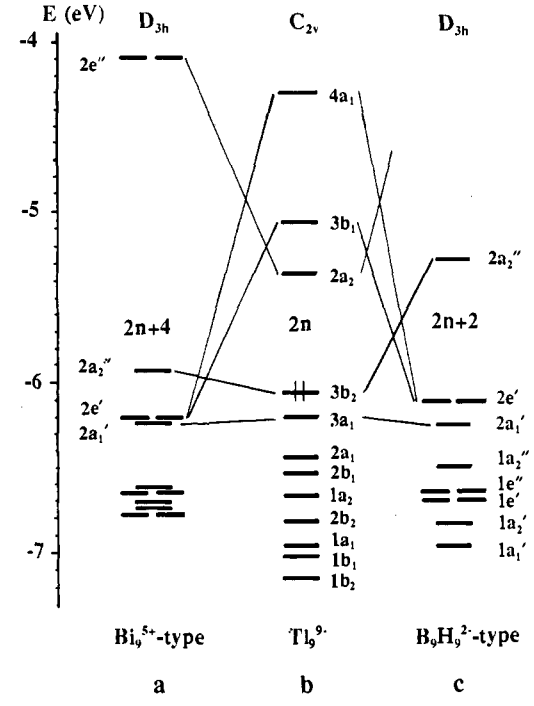

Figure 5. The MO diagram for predominantly p-based orbitals in the observed (C_{2v}) Tl_9^{9-} cluster (b) relative to those for idealized D_{3h} versions proportional as Bi_9^{5+} (a) and $B_9H_9^{2-}$ (c). The last two differ because of the relative heights of the trigonal prisms.

calculated for the observed cluster is 0.70 eV with a $3b_2$ HOMO orbital at –6.06 eV, reasonably close to that for the Tl_5 cluster (–5.95 eV).

Referring to Figures 2a and 3, the real C_{2v} geometry is reached through compression of the 1-1 pair of atoms as well as stretching of 3-3 and both 4-4 separations of the hypothetical Bi_9^{5+}-like model, together with the changes associated with movement of Tl2 toward the center of the rectangular face defined by the Tl4 atoms. Motions of the pair of Tl3 atoms, like those of Tl2, can be viewed as following the changes in prism edges to maintain reasonable Tl–Tl distances. Overlap population analyses reveal that the bonding 2e′ in the Bi_9^{5+} model is split into strongly antibonding $3b_1$ and $4a_1$ orbitals upon such distortion because both have interactions that are bonding along the elongated 4-4 and antibonding along the new 2-3 contacts. Although the stretching of 3-3 decreases antibonding interactions in $3b_1$, this influence is totally covered up by increased antibonding contribution along the 3-4 edges. The $4a_1$ is further destabilized by increased out-of-phase interactions between Tl2 and the Tl4 face atoms. The resultant $2a_2$ LUMO contains dominant contributions from Tl4 atoms that are antibonding along all four edges, while the $3b_2$ HOMO exhibits in-phase interactions within both 1-4-4 triangular faces but out-of-phase components along the three prismatic edges. The $3b_2$ orbital is also the highest bonding member according to total overlap populations. Thus, after assignment of the nine low-lying, mainly s-based orbitals to the thallium atoms, the calculation predicts nine bonding skeletal MOs as observed for the Tl_9^{9-} cluster anion. Comparable distortions of the more distance $B_9H_9^{2-}$-like geometry, which is already $2n + 2$, to gain Tl_9^{9-} are a little more complex (Figure 5c) because a third $2a_2''$ (LUMO) orbital also becomes the bonding $3b_2$ HOMO on pronounced elongation of two Tl4–Tl4 edges; the 2e′ sets in both D_{3h} cases naturally behave similarly on distortion.

The basic point concerning the observed distortion is that, analogous to those perceived in K_8In_{11}[7] and A_8Tl_{11} (A = K, Rb, Cs),[6] the pronounced displacement of Tl2 along the 2-fold axis toward the rectangular prismatic face greatly increases the antibonding interactions between that atom and all neighbors in the $4a_1$ and $3b_1$ representations, thereby emptying these orbitals and again giving a hypoelectronic result. Four new contacts are established for Tl2 at the expense of two 4-4 "bonds". Electronic reasons why the opening face is not instead expanded to a C_{4v} square are probably because such motions would leave the Tl4 atoms only three-bonded in a loosely connected cluster. In fact, Tl2 behaves as a quasi-interstitial atom in holding the cluster together, as better exemplified by the more symmetric $K_8Tl_{10}Zn$[6] analogous to $K_8In_{10}Zn$.[9]

The electronic state of Tl_9^{9-} may also be easily recovered by vertex removal from a closo-polyhedron rather than through distortion of another nine-atom polyhedron. The classic (Wade's rule) icosahedral Tl_{12}^{14-} will contain 13 skeletal bonding (p) orbitals, and centering it by a Tl^{3+} ion gives the closed shell Tl_{13}^{11-}.[6] The process introduces no new bonding orbitals, rather, the interstitial's orbitals simply increase bonding in the existing MOs. This step is very similar to those already described for the heteroatom centering steps in $In_{10}Ni^{10-}$ ($\sim C_{3v}$)[30] and $In_{10}Zn^{8-}$ (D_{4d}).[9] The Wade's rules vis-a-vis arachno, hypho, etc. products are violated when two or more adjacent vertices are removed. Loss of electron pairs as well as surface-bonding skeletal orbitals is usually observed, but the number of electrons lost strongly depends on the number and geometric distribution of the missing atoms. Along the lines of the prophetic calculations of Burdett and Canadell,[35] our EHMO results indicated that in the conversion of Tl_{13}^{11-} directly to the closed shell, observed Tl_9^{9-} occurs simply through the removal of the indicated four adjoining vertices along with three skeletal electron pairs. In other words, three skeletal bonding orbitals are lost. The process can also be described in the other order: loss of the four vertices from Tl_{12}^{14-} along with three skeletal (p) pairs gives the hypothetical, closed shell Tl_8^{12-}, and addition of Tl^{3+} along the 2-fold axis (Tl2) gives the observed Tl_9^{9-}. Although this is a less "chemical" process than the distortion or centering, or both, that we have previously encountered, vertex removal with minimal rearrangements must be viewed as yet another means whereby high charges can be reduced and hypoelectronic clusters stabilized. Of course, the problems of generating a stable, well bonded solid structure also play obvious roles in what may be accessed.

The electron distribution in the phase $Na_2K_{21}Tl_{19}$ can thus be described as follows. Each formula unit contains two Tl_5^{7-} and one Tl_9^{9-} clusters, which require altogether $2 \times 22 + 36 = 80$ valence electrons. Since each Tl atom has three valence electrons and each alkali metal atom, one, the number available is $19 \times 3 + 23 \times 1 = 80$, making the title compound electron-precise with a probable closed-shell structure and diamagnetic properties, as observed. Its high specific resistivity ($\rho_{293} \sim 800\ \mu\Omega$·cm) supports the extreme electron localization, although the possibly complex temperature dependencies below room temperature (above) will require more work to interpret. High resistivities with conflicting temperature dependencies have been found for other compounds containing what are predicted to be closed-shell clusters, e.g., Na_2In,[36] β-NaSn,[37] $K_8In_{10}Zn$,[13] and $K_8In_{10}Hg$.[38] These weak conductivity effects may result from semimetal characteristics, a condition that does not conflict with the spirit of Zintl (valence) phase assignments.

It is interesting to note that Tl_9^{9-} affords a second example (beyond Tl_6^{6-}) with which one might model the unusual neutron diffraction effects observed for a K–Tl melt at the 1:1 composition,[39] which is also at the maximum in melt resistivity. A sharp peak with a remarkably short 0.77 $Å^{-1}$ wavevector corresponds to intercluster separations of the order of 9.3 to 10 Å. For

(35) Burdett, J. K.; Canadell, E. *Inorg. Chem.* **1991**, *30*, 1991.
(36) Sevov, S. C.; Corbett, J. D. *J. Solid State Chem.* **1992**, *103*, 114.
(37) Nesper, R. Private communication.
(38) Sevov, S. C.; Ostenson, J. E.; Corbett, J. D. *J. Alloys Comp.* **1993**, *202*, 289.
(39) Xu, R.; Verkerk, P.; Howells, W. S.; de Wijs, G. A.; van der Horst, F.; van der Lugt, W. *J. Phys.: Condensed Matter* **1993**, *5*, 9253.

comparison, the shortest (center-to-center) cluster separation in the Tl_9^{9-} layers at room temperature (Figure 4a) is 8.94 Å, which becomes 9.3 Å with an estimated 4% expansion in the melt at 350 °C. Even Tl_{12}^{14-} or Tl_{13}^{11-} polyhedra cannot be readily excluded as models. Of course, the solids isolated from these systems also represent the most effective ways of simultaneously fitting space, solvating or bonding cluster anions with cations, and meeting electronic requirements, and there obviously is no assurance that the species found in crystalline solids are predominant in the liquid state. The long range order in the melt suggested by the above diffraction results also imply strong and specific cation–polyanion bonding (or solvation) effects in the liquid state, as have been inferred in many solid structures.

Although a few examples of classical (Wade's rule) clusters are now known in the solid state for the heavier triel (group 15) elements In and Tl, e.g., the smaller Tl_4^{8-} and Tl_5^{7-}, these elements generally appear to be too electron-poor to allow formation of classical isolated clusters with what would ordinarily be unfavorably high anionic charges. But, we have now seen several examples of how either distortions with or without interstitial atoms or vertex losses may avoid these problems in hypoelectronic examples, namely Tl_{11}^{7-}, Tl_9^{9-}, and Tl_6^{6-}. Clearly another way to stabilize discrete polyanions containing electron-poor elements like thallium is in combination with electron-richer elements in heteroatomic polyanions such as in the $TlSn_9^{3-}$ and $TlSn_8^{3-}$ ions obtained via molecular solvent routes.[40] Yet another way to stabilize a product is through intercluster exo bonds within three-dimensional networks, each intercluster bond reducing the formal charge on each unit by one, nominally by oxidizing the s-pair.[13] We have found many examples of this for indium, and networks appear to be the predominant feature with gallium.[41] Again, the thallium results are in part pleasantly divergent from the characteristics of the lighter elements inasmuch as isolated and novel clusters appear in the majority of alkali metal–thallium phases. A few unusual networks have been found, for example, in (a) a combination of both isolated and condensed pentacapped trigonal prismatic Tl_{11} ($\sim D_{3h}$) units and (b) condensed icosahedra alone or with hexagonal antiprisms, but no analogues of known gallium or indium network structures so far. The variations and versatilities possible among these elements are both stimulating and challenging.

Acknowledgment. We are indebted to S. C. Sevov for calling the close relationships between Tl_9^{9-} and the iscosahedral Tl_{12}^{14-} to our attention. J. Ostenson measured the magnetic data for us. The Ames Laboratory is operated for U.S. Department of Energy by Iowa State University under Contract No. W-7405-Eng-82. This research was supported by the Office of the Basic Energy Sciences, Materials Sciences Division, DOE.

Supplementary Material Available: Tables of crystallographic details and positional and anisotropic displacement parameters for $Na_2K_{21}Tl_{19}$ and drawings of the cation distributions about the two clusters (5 pages). This material is contained in many libraries on microfiche, immediately follows this article in the microfilm version of the journal, and can be ordered from the ACS; see any current masthead page for ordering information.

(40) Burns, R. C.; Corbett, J. D. *J. Am. Chem. Soc.* **1982**, *104*, 2804.
(41) Belin, C.; Tillard-Charbonnel, M. *Prog. Solid State Chem.* **1993**, *22*, 59 and references therein.